National Journal of Advanced Research
ISSN: 2455-216X; Impact Factor: RJIF 5.12
Received: 07-08-2019; Accepted: 10-09-2019
www.allnationaljournal.com
Volume 5; Issue 4; October 2019; Page No. 64-69

Study of dielectric and magnetic properties of bismuth lanthanum titanium oxide synthesized by semi wet route

Pooja Gautam[1*], Arvind Kumar Bharti[2]
Department of Chemistry, Modern Institute of Technology and Research Center, Tijara road Alwar Rajasthan, India

Abstract
Bismuth lanthanum titanate, $Bi_3LaTi_3O_{12}$ (BLTO) ceramic was fabricated semi-wet route. The single phase formation of BLTO was confirmed by X-ray diffraction pattern. The complexation of citric acid with oxygen metal bond was found out by FT-IR studies in the calcined powder at 800 °C for 6 h. Transmission electron microscope (TEM) analysis is used to determine the particle size in the range of 212 ± 20 nm. The average grain size obtained from scanning electron microscope (SEM) and atomic-force microscope (AFM) was almost have the similar values 200 ± 20 nm and 217±20 nm. The surface roughness and root means square roughness was found to be 46.015 and 58.661 nm, from the AFM analysis. Magnetic properties of ceramic show the magnetic transition of anti-ferromagnetic to ferromagnetic nature in the M-H and M-T curve. The blocking temperature and Neel's temperature was found to be 155 K and 51 K respectively. The dielectric constant (ε') value of $Bi_3LaTi_3O_{12}$ ceramic was found to be 403 at 100 Hz at 500 K.

Keywords: semi-wet route; dielectric properties; magnetic behavior

Introduction
Bismuth lanthanum titanate, $Bi_3LaTi_3O_{12}$ (BLTO) was showing the great interest in research of ferroelectric materials due to their technological application in sensors, actuators and nonvolatile random access memories (NRAM) ferroelectric. Lead-based ferroelectric materials such as Pb (Zr, Ti) O_3 (PZT) were the most widely used piezoelectric materials because of their better electrical properties [1]. The high remnant polarization of PZT at low temperature made it a dominant material for memory devices presently being used in ferroelectric random access memory (FRAM) [2, 3]. However, these material has shown drawbacks of fatigue, leakage current and aging [4, 5]. Additionally, PZT has high lead content. The evaporation of toxic lead during fabrication of the ceramics may cause the major health and environment problems in the long term. In addition, there is also a desire to restrictions the integration of lead containing materials in to electronic devices, the bismuth based layered ferroelectrics are environment friendly. Lead-free bismuth layer-structured ferroelectric thin films, such as $SrBi_2Ta_2O_9$ (SBT) and $Bi_4Ti_3O_{12}$ (BTO) have been confined in the usual industrial application due to its small polarization and high processing temperature [6, 7]. BTO has been copiously studied because of their better strain resistance on common Pt electrodes [8] and large spontaneous polarization (P_s), low processing temperature and high Curie temperature (T_c = 675 °C) [9]. Its layered structure belongs to the Aurivillius family having desirable electrical and electromechanical properties [10, 12]. Furthermore, there is a rising the demand to succeed the lead based material and develop a new lead free material. La-doped BTO exhibited low processing temperature and large value of remnant polarization [13, 15]. It is also significant with Si-based integrated circuit technology.
In the past, few literature of BLTO compound mostly explains thin film and ferroelectric behavior but in this manuscript, we have synthesized BLTO ceramic first time fabricated via semi wet route at low temperature. This method has many advantages than other methods such as conventional solid state method and sol-gel methods because this method is simple and carries out using metal nitrate solutions and solid TiO_2. It is simpler as compared to the solid state method because solid state method contains several multi-steps (i.e., intermediate grindings, drying, etc.) to get precursor powder. On the other hand, in the case of sol-gel methods a very costly alkoxide of titanium is used as Titanium source. In the present work, we have used the cheap solid TiO_2 as Titanium source which was directly added to the metal nitrate solution to get BLTO precursor powder on combustion. This fabrication route shows the enhancement in dielectric and magnetic properties. The aim of the present work is to examine the dielectric and magnetic behavior of the $Bi_3LaTi_3O_{12}$ ceramic fabricated by semi-wet route. The ceramic has been characterized by various techniques, XRD, TEM, SEM and AFM analysis.

Experiment
$Bi_3LaTi_3O_{12}$ceramic was fabricated by the semi-wet route. The analytical grade chemicals of Bismuth nitrate, Bi $(NO_3)_3.5H_2O$ (99.5%, Merck, India), Lanthanum oxide, La_2O_3 (99.0%; Merck, India), titanium oxide, TiO_2 (99.9%, Merck, India) were taken in stoichiometric ratio. The solutions of Bi $(NO_3)_3.5H_2O$ was prepared using distilled water and La_2O_3 dissolved in dilute nitric acid. Both the solutions were mixed in a beaker. The solid TiO_2 in form of powder was added to the solution. A calculated amount of citric acid equivalent to the metal ions was dissolved in water and added in the heterogeneous mixture. The resultant heterogeneous mixture was heated on a hot plate using magnetic stirrer at 70-80 ºC to evaporate water. The residual mass was dried at 100-120 ºC in hot air oven. The BLTO dried powder was calcined at 800 ºC for 6 h in a muffle

furnace and ground into a fine powder using poly vinyl alcohol (PVA) as a binder in a mortar and pestle. Cylindrical pellets (11.6mm x 1.00mm) were made using a hydraulic press. The pellets were sintered at 900 ºC for 8 h.
The crystalline phase of sintered sample was identified by X-ray diffractometer (Rigaku Miniflex 600, Japan) using CuK_{α} as X-ray source with a wavelength of 1.54 Å. The FT-IR spectra of calcined powder of BLTO ceramic was recorded by an ATR-FTIR spectrophotometer (Bruker, ALPHA model) in the range from 4000 - 500 cm^{-1}. The bright field TEM image of the ceramic was examined using a transmission electron microscope (TEM, FEI TECANI G2 20 TWIN, USA). The microstructure of the fractured surfaces of pellet was examined by using a scanning electron microscope (ZEISS, model EVO18 research, Germany). The elemental analysis of the sintered sample of BLTO was performed by EDX (Oxford instrument; USA) attached with the SEM unit. The surface morphology and roughness of BLTO ceramic were examined using atomic force microscopy (NTEGRA Prima, Germany). Temperature and field-dependent dc magnetization of ceramic were measuredby using Magnetic Property Measurement System Quantum Design MPMS-3, over a temperature range 2–300 K at a magnetic field of 7 tesla. The temperature variation of field cooled (FC) and zero field cooled (ZFC) magnetization at 100 Oe applied field were carried out using SQUID VSM dc magnetometer. The dielectric data of BLTO ceramic pellets coated with silver paints were collected using the LCR meter (PSM 1735, Newton 4thLtd, U. K.) with the variation of frequency (100 Hz – 5 MHz) and temperature (300-500 K).

Results and Discussion

Figure 1, displayed XRD patterns of BLTO calcined at 800 ºC for 6 h and sintered pellet at 900 ºC for 8 h. XRD pattern of calcined powder and sintered pellets are identical to each other which reveal the same phases. On analysis the XRD peaks, it was observed the single phase formation of $Bi_4Ti_3O_{12}$ as per JCPDS card No. 89-750.

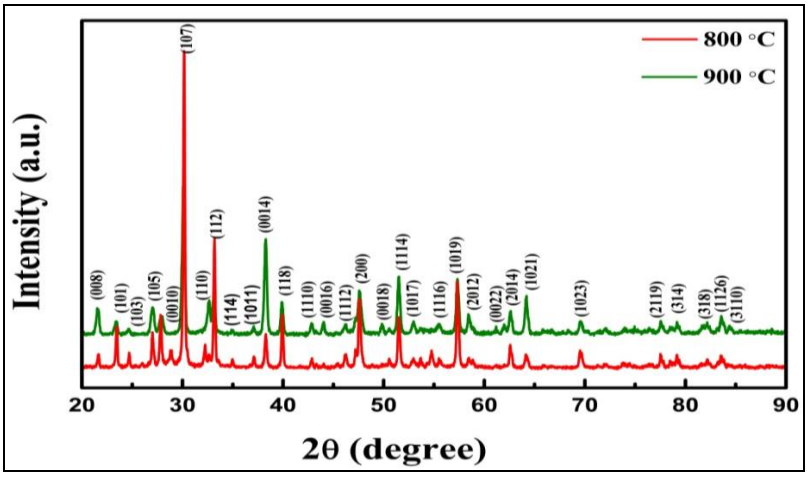

Fig 1: XRD patterns of $Bi_3LaTi_3O_{12}$ ceramic (a) Sintered at 900 °C for 8 h and (b) calcined at 800 °C for 6 h.

Figure 2, shows the Fourier transform infrared (FT-IR) spectrum of BLTO calcined powder at 800 °C for 6 h. The most of the citrate group disappears during the combustion process. The peaks observed at 410, 592 and 836 cm^{-1} for the calcined powder because of bending and stretching mode of Ti-O-Ti and Ti-O band [16, 17]. The peak observed at 1639 cm^{-1} could be designated to the OH vibrational mode of the absorbed water molecule [18]. Oxygen–metal bonds band characteristics were usually exhibited in the 400–850 cm^{-1} [19, 20].

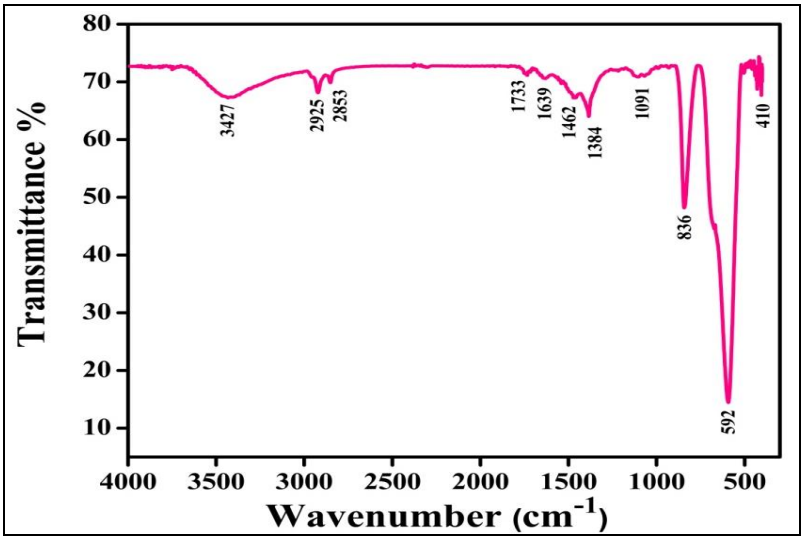

Fig 2: FITR spectra for the $Bi_3LaTi_3O_{12}$ ceramic calcined at 800 °C for 6 h.

Figure 3a shows transmission electron microscopy (TEM) bright field images of the BLTO ceramic. The shape of the particle was found to be spherical and platelet like. The average particle size was observed in the ranges of 212 ± 20 nm. Figure 3b shows microstructure of the fracture surface observed from the scanning electron microscopy. The SEM image exhibits flake like and platelet type bimodal grains [21]. The average grain size of the BLTO ceramic was observed in the range of 200 ± 20 nm. The EDX spectrum of BLTO ceramic for grain and bulk are showing in Figure 4a&b. The atomic and weight percentage of the constituent elements in BLTO ceramic for grain and bulk were found to be nearly the same value. The atomic percentages of Bi, La, Ti and O, at a grain as marked in the Fig. 4a were found to be 13.56, 10.93, 17.22 and 58.30, respectively. The atomic percentage of Bi, La, Ti, and O, at bulk (Fig. 4b) was found to be 13.25, 11.30, 15.72, and 59.73 respectively. These results clearly show the existence of Bi, La, Ti and O as per the stoichiometric ratio in BLTO ceramics which confirmed the purity of the material [22, 23].

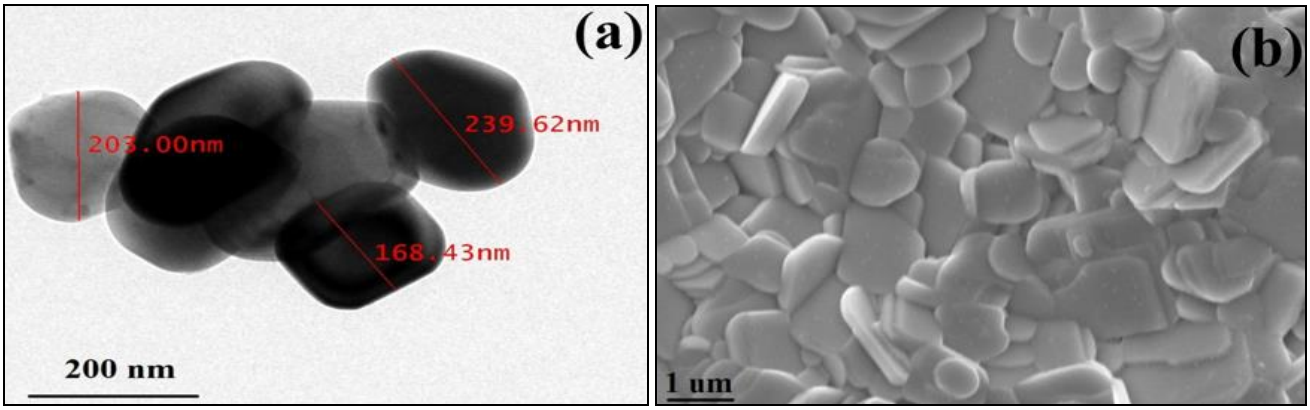

Fig 3: (a) Bright field TEM image (b) SEM morphology of fractured surface of $Bi_3LaTi_3O_{12\ ceramic}$ sintered at 900 °C for 8 h.

The AFM image of BLTO ceramic shows the surface morphology of grains and grain boundary for a two-dimensional image in Figure 5a. It exhibited compact structure with granular morphology with clear grain boundary. Figure 5b shows three-dimensional AFM image which indicates the maximum area peak height of the grain to be 179.98 nm within the scan area of 3.0 µm × 3.0 µm. Figure 5c shows the three-dimensional surface roughness of BLTO ceramic. The average roughness and root mean square roughness of the ceramic were found to be 46.015 nm and 58.661 nm, respectively. The AFM analysis revealed the presence of the particles with the broad size distribution in the BLTO ceramic [24]. The average grain size determined for two-dimensional was found to be 217 ± 20 nm out of 128 grains as shown in the histogram Figure 5d. The result of TEM, SEM and AFM analysisare always supportto each other.

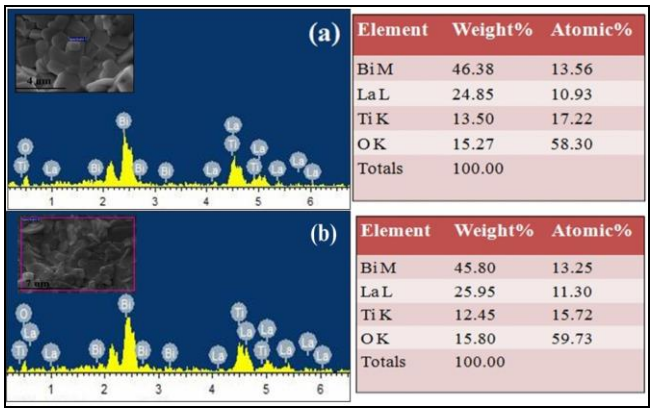

Fig 4: (a) EDX spectra of grain and (b) grain boundaries of $Bi_3LaTi_3O_{12}$ ceramic sintered at 900 °C for 8 h.

Figure 6a shows the magnetization behavior of BLTO ceramic as a function of temperature. The hysteresis loop of zero-field cooling (ZFC) and field cooling (FC) measured in the temperature range 2-300 K at the applied field of 100 Oe. The ZFC shows a cups and bifurcation with the corresponding to FC curve below 300 K. It was often present in a gathering of ferromagnetic like particle exhibiting super magnetic above a certain temperature. The cups in ZFC curve defined the blocking temperature [25]. The blocking temperature is found to be 155 K. On the other hand, the FC curve shows hump like a minor peak at 51 K. The temperature knows as Neel's temperature. It appears to be an anti-ferromagnetic and ferromagnetic moment. The ceramic shows both type behavior, blocking temperature and Neel's temperature of ZFC and FC curve by bimodal size distribution corresponding to TEM images.

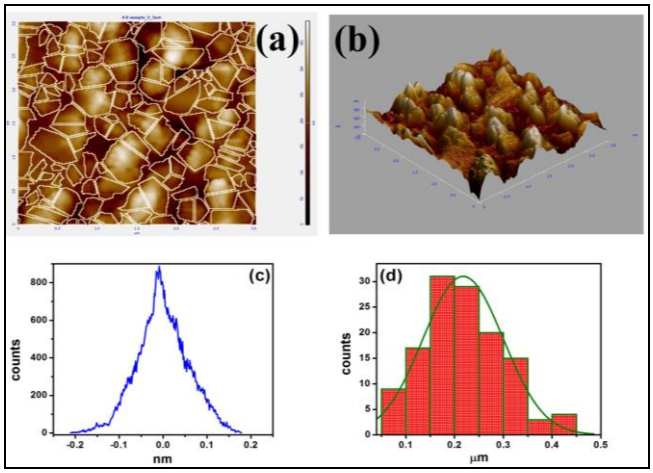

Fig 5: AFM images of $Bi_3LaTi_3O_{12}$ Ceramic sintered at 900 °C for 8 h (a) two-dimensional image showing grains and grain boundaries (b) three-dimensional image exhibited high peak distribution (c) Histogram of three-dimensional particle roughness and (d) Particle size distribution curve.

The large particle explains to Neel's temperature and blocking for the smaller particle size [26]. Figure 6b

displayed the magnetization as a function of magnetic field measured at 7 T for the BLTO ceramic. The magnetization curves show no perfect saturation and it has been situated even at a magnetic field of 7 T at room temperature. It is observed that BLTO ceramic shows anti-ferromagnetic and weak ferromagnetic in nature. The coercivity shows open hysteresis loop approximate at 72 Oe as shown in the inset figure. The apparent opening has been exhibited in the curves indicating the presence of ferromagnetic moment. This weak ferromagnetic moment arises due to spin canting of the atomic magnetic moments and could not be compensated spin at the surface of BLTO ceramic [27, 28].

The temperature dependence of the dielectric constant (ε') and loss tangent for the BLTO ceramic at few selected frequencies (100 Hz, 1 kHz, 10 kHz and 100 kHz) is shown in Figure7.

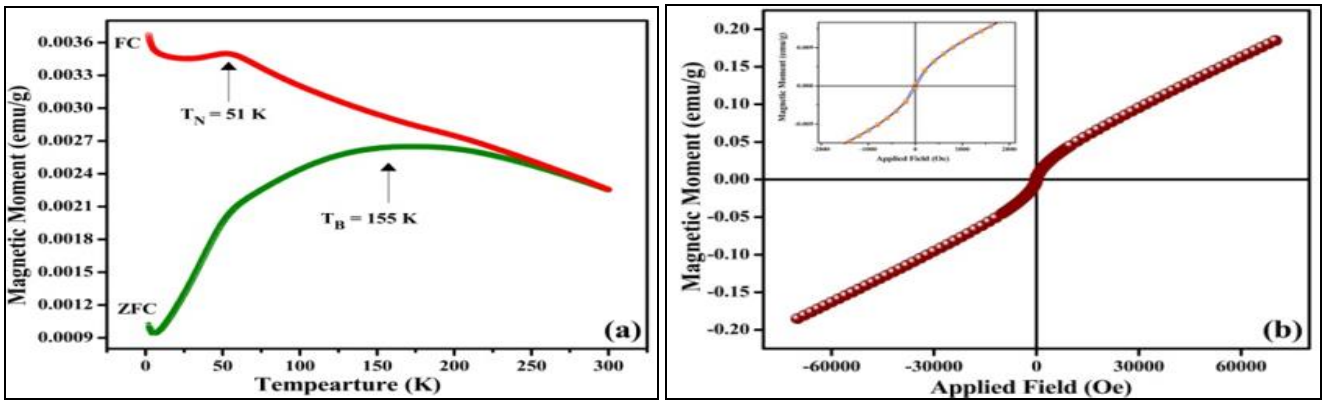

Fig 6: (a) Temperature-dependent zero field cooled (ZFC) and field cooled (FC) magnetization measured at H = 100 Oe and (b) magnetization versus applied field at 300 K for the Bi3LaTi3O12 ceramic.

It is observed from the Figure **7**a that the dielectric constant of BLTO ceramic is independent of behavior up to 400 K and then increases slowly. The value of ε' was progressively decreases with increasing frequency at a given temperature. The dielectric constant of BLTO ceramic was observed 405, 337, 211 and 153 at 100 Hz, 1 kHz, 10 kHz and 100 kHz respectively; at 500K. Temperature dependence of loss tangent (tanδ) of the BLTO ceramic is shown in Figure**7**b. The tanδ is strongly temperature dependent and it increases with decrease in frequency. The value of tanδ is lowest (0.076) at 100 kHz and 500 K.

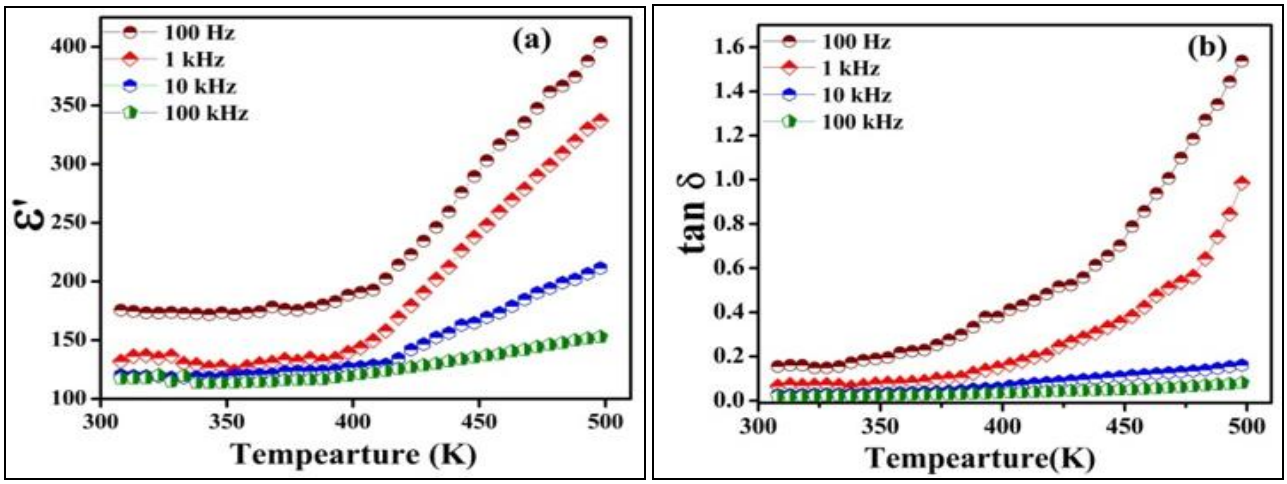

Fig 7: Plot of (a) Dielectric constant and (b) tan δ as a function of temperature for $Bi_3LaTi_3O_{12}$ ceramic sintered at 900 °C for 8 h.

Figure8 shows the variation of dielectric constant (ε') and loss tangent (tanδ) with frequency at few selected temperatures. It is observed from Figure 8a, the dielectric constant increases with decrease infrequency. The high value of the dielectric constant at low frequency region is due to the existence of space charge polarization in the ceramic [29, 30].

The low value of the dielectric constant at higher frequencies is important for the ferroelectric and electro-optic devices.

Frequency dependent dielectric studies show the low freque ncy relaxation is associated with the entity of barrier layers at the electrode and the high frequency region with the entity of barrier layers at grain boundaries.

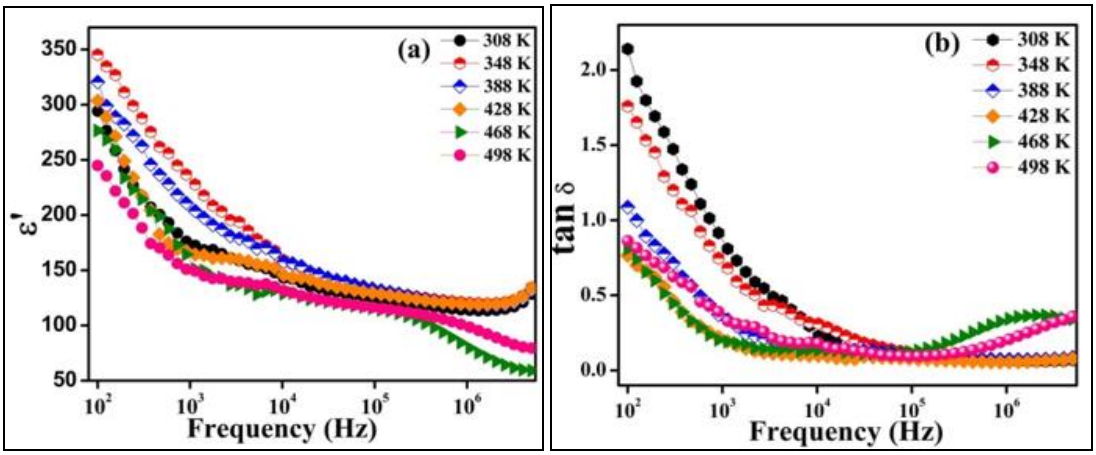

Fig 8: Plot of (a) Dielectric constant and (b) tan δ as a function of frequency for $Bi_3LaTi_3O_{12}$ ceramic sintered at 900 °C for 8 h.

Figure 8b shows decreases of tan δ with increasing frequency at few selected temperature. The lowest value of tan δ was found to be 0.75 at 428 K. The relaxation peaks in tanδ were observed at high frequency regions. The above dielectric characteristic behavior of a ferroelectric relaxor material is usually characterized by diffuse phase transition and strong relaxational dispersion in dielectric constant and tan δ indicating the thermally activated relaxation. In both the curves, the dielectric constant and loss tangent increases with decreasing frequency, which is the common feature of polar dielectric materials.

Conclusions

$Bi_3LaTi_3O_{12}$ceramic was fabricated by semi-wet route at low temperature. The single phase formationof the BLTO was confirmed by XRD. The average particle size of the BLTO ceramic wasobserved 212 ± 20 nm by TEM analysis. The Ti-O and Ti-O-Ti band stretching frequency were confirmed by FT-IR in the BLTO ceramic calcined at 800 °C. The SEM study of BLTO ceramic sintered at 900 °C for 8 h exhibited average grain size 200 ± 20 nm and with clear grain boundary which was also substantiated by AFM study. EDX spectrum displayed the presence of Bi, La, Ti and O elements in the ceramic. The atomic percentage of Bi, La, Ti and O elements were observed 13.25, 11.30, 15.72, and 59.73, respectively. The atomic percentage are inconsistent with stoichiometric of BLTO ceramic which confirms the purity of synthesized BLTO ceramic. Root mean square roughness and average roughness of the ceramic were found to be 58.661 and 46.015 nm, respectively. The presence of blocking and Neel's tempearture in the BLTO ceramic explain the biomodal particle size distribution. Frequency dependent dielectric studies show the low freque ncy relaxation is associated with the entity of barrier layers at the electrode and the high frequency region with the entity of barrier layers at grain boundaries.

Acknowledgments

One of the authors Pooja Gautam is grateful to IIT (BHU) for financial support (Grant No.13051009) as teaching assistantship. Authors are thankful to Central Instrument Facility Centre (CIFC) IIT (BHU) for Providing SEM, TEM, EDX and Magnetic properties analysis.

References

1. Jaffe B, Cook WR, Jaffe H. Piezoelectric Ceramics, Academic Press, London, New York, 1971.
2. Scott JF, Araujo PD, Carlos A. Ferroelectric Memories. Science, 1989; 246:1400.
3. Zhang QQ, Gross SJ, Tadigadapa S, Jackson TN, Djuth FT, Mckinstry ST. *et al*. Sens. And Actu. A, 2003; 105:91.
4. Chang JF, Desu SB, Mater J Res. 1994; 9:955-969.
5. Warren WL, Dimos D, Tuttle BA, Pike GE, Schwartz RW, Clews PJ. *et al*. J Appl. Phys. 1995; 77(12):6695-6702.
6. Lettieri J, Zurbuchen MA, Jia Y, Schlom DG, Streiffer SK, Hawley ME. *et al*. Appl. Phys. Letter. 2000; 76:2937-2939.
7. Lee HN, Visinoiu A, Senz S, Harnagea C, Pignolet A, Hesse D. *et al.* J Appl. Phys. 2000; 88:6658-6664.
8. Park BH, Kang BS, Bu SD, Noh TW, Lee J, Jo W. *et al*. Nature. 1999; 401:682-684.
9. Liu W, Wang X, Tian D, Xiao C, Wei Z, Chen S. Mater. Sci. Appli. 2010; 1:91-96.
10. Fang P, Fan H, Xi Z, Chen W. Solid State Commu. 2012; 152:979-983.
11. Ahn CW, Jeong ED, Kim YH, Lee JS, Lee HJI, Kim WJ. *et al*. Electroceramic. 2009; 23:402-405.
12. Subbarao EC. J Phys. Chem. Solid. 1962; 23:665-676.
13. Kojima S, Hushur A, Jiang F, Hamazaki S, Takashige M, Jang MS, Shimada S. *et al*. J Non- Cryst. Solid. 2001; 293-295:250-254.
14. Pavlovic N, Koval V, Dusza J, Srdic VV. Ceram. Int. 2011; 37:487-492.
15. Rachna S, Bhattacharyya S, Gupta SM, Mater. Sci. Eng. B. 2010; 175:207-212.
16. Devi RS, Venckatesh R, Sivaraj R. Int. J Innov. Res. Sci. Eng. Technol. 2014; 3:15206-15211.
17. Gautam P, Khare A, Sharma S, Singh NB, Mandal KD. Prog. Nat. Sci. Mater. Inter. 2016; 26:567-571.
18. Ocwelwang AR, Tichagwa L. Int. J Adv. Res. Chem. Sci. 2014; 1:28-37.
19. Simoes AZ, Quinelato C, Ries A, Stojanovic BD, Longo E, Varela JA. Mater chem. and Physi. 2006; 98:481-485.
20. Feng H, Zijun H, Junlin X, Yuhui L. J of Anal. Chem. 2014; 5:1142-1150.

21. Roy M, Bala I, Barbar SK, Jangid S, Dave P. J Phys. Chem. Solid. 2011; 72:1347-1353.
22. Singh L, Rai US, Mandal KD, Rai AK. Appl. Phys. A. 2013; 112:891-900.
23. Prakash BS, Varma KBR. J Mater. Science. 2007; 42:7467-7477.
24. Gautam P, Yadava SS, Khare A, Mandal KD. Ceram. Inter. 2017; 43:3133-3139.
25. Lihua C, Meicheng L, Zipei W, Lei D, Dandan S, Shangyi D. *et al*. Eng. Comm. 2014; 00:1-6.
26. Mendonça EC, Jesus CBR, Folly WSD, Meneses CT, Duque JGS, Coelho AA. *et al*. J Appl. Phys, 2012; 111:053917.
27. Babu GA, Hayakawa Y, Ravi G. Mater. Letter. 2015; 149:54-57.
28. Chaudhuri A, Mandal K. Mater. Reser. Bulle. 2012; 47:1057-1061.
29. amurugaraj PB, Suresh S, Koteeswari P, Mani P, J Mater. Phys. Chem. 2013; 1:4-8.
30. Ponpandian N, Balaya P, Narayanasamy A. J phys. Condens. Matter, 2002; 14:3221.